Structural Engineering International

ISSN: (Print) (Online) Journal homepage: https://www.tandfonline.com/loi/tsei20

Influence of Beam-to-Column Connections in the Seismic Performance of Precast Concrete Industrial Facilities

Hugo Rodrigues Prof., Hugo Vitorino PhD Student, Nádia Batalha PhD Student, Romain Sousa Dr, Paulo Fernandes Prof. & Humberto Varum Prof.

To cite this article: Hugo Rodrigues Prof., Hugo Vitorino PhD Student, Nádia Batalha PhD Student, Romain Sousa Dr, Paulo Fernandes Prof. & Humberto Varum Prof. (2022) Influence of Beam-to-Column Connections in the Seismic Performance of Precast Concrete Industrial Facilities, Structural Engineering International, 32:4, 507-519, DOI: 10.1080/10168664.2021.1920082

To link to this article: https://doi.org/10.1080/10168664.2021.1920082

Influence of Beam-to-Column Connections in the Seismic Performance of Precast Concrete Industrial Facilities

Hugo Rodrigues, Prof.; **Hugo Vitorino**, PhD Student , RISCO, Civil Engineering Department, University of Aveiro, Aveiro, Portugal; **Nádia Batalha**, PhD Student , CONSTRUCT-LESE, Faculty of Engineering (FEUP), University of Porto, Porto, Portugal; **Romain Sousa**, Dr , CDRSP, Polytechnic Institute of Leiria, Leiria, Portugal; **Paulo Fernandes**, Prof. , CERIS, ESTG - Polytechnic Institute of Leiria, Leiria, Portugal; **Humberto Varum**, Prof. , CONSTRUCT-LESE, Faculty of Engineering (FEUP), University of Porto, Porto, Portugal. Contact: hrodrigues@ua.pt
DOI: 10.1080/10168664.2021.1920082

Abstract

Past earthquakes have brought attention to the poor performance of precast reinforced concrete structures, especially relating to beam-to-column connections. The evaluation of different methodologies for the analysis of beam-to-column connections in industrial buildings is important. In the present work numerical analyses developed allowed the study of the effect that different story heights and connection properties have on frequencies, drifts, seismic coefficients and connection sliding. The results showed that the friction between concrete elements and the consideration of neoprene have a small impact on the drift demands in the columns and the seismic coefficients of the structures analyzed; on the other hand, the effect of steel dowel on the drift demands and seismic coefficients is significant. The comparison of models with different properties and connections allowed a better understanding of the parameters that affect the seismic behavior of precast reinforced concrete buildings the most and provide indications for building more accurate and efficient numerical models.

Keywords: industrial buildings; precast reinforced concrete; beam-to-column connections; seismic performance; numerical analysis

Introduction

Precast reinforced concrete (PRC) structures have shown poor seismic performance in several cases, presenting damage to structural and non-structural elements, and highlighting the vulnerability of industrial buildings. [1, 2–7] An important part of these buildings was not designed with seismic concerns. Most of the observed damage is related to structural elements, namely in the beam-to-column connections. Several buildings have shown significant failures and collapse. For example, in the Emilia earthquake of 20 and 29 May 2012, more than half of the existing precast structures exhibited significant damage. [8–10] Even in moderate and short duration earthquake events, PRC structures exhibit high levels of structural damages, as described in Ref. [11] after field observations of the 2011 Lorca earthquake. The continuing reports of damage to precast structures derived from seismic events pointed to a need for consistent methodologies for analysis, modeling and assessment of existing constructions. Those models need to account for the interaction between structural elements (e.g. beam-to-column connections) and both structural and non-structural elements in order to describe the nonlinear dynamic behavior of this type of structure. [12–15] Ref. [16] developed a numerical model of a PRC building with an earthquake analysis and experimental validation; the model was developed with fiber-based finite elements of a half-scale 3D PRC frame tested under dynamic conditions. The nonlinear analyses allowed the prediction of the building behavior to a good approximation, especially in terms of story displacements. The need to assess the seismic vulnerability of existing buildings led different authors to develop new modeling solutions following both macro (e.g. Refs. [17–20]) and refined numerical models (e.g. Refs. [21–23]). The use of refined models tends to offer more precise results, given their ability to consider the different mechanisms involved. However, these models are computationally demanding and therefore unsuitable for common engineering applications or seismic risk analysis on the scale of large buildings. Since beam-to-column connections were identified as one of the most critical elements in precast structures under seismic loads, some work has been developed in this field over recent years. The work in Refs. [19, 20] should be highlighted, which focused on the behavior of connections without dowels; others, e.g. Ref. [17], account only for the contribution of dowels. The macro-element used in the present work follows the same general concepts adopted in Ref. [24] i.e. explicitly modeling the contribution of both friction and dowel action, but the present authors attempt here to introduce more precise friction and dowel models, being developed and validated based on past experimental tests. [1]

The main research objectives of this study are to understand the influence of several parameters affecting the seismic response on common PRC structures, namely earthquake type, story height and vertical roof loads. The contribution is also studied of the different mechanisms present in beam-to-column connections, such as dowels, neoprene pads and friction between the elements, in the overall response of the structure. The results obtained can help the definition of modeling strategies, and numerical assumptions in the design and assessment of existent PRC, in order to represent the damage found in this type of building.

Description of the Case Study

The PRC building under study represents an existing industrial framed structure (*Fig. 1*) constituted by one floor with an area of 180×175 m^2 and a height of 12 m. The structure has 5 spans in the *X*-direction (*Fig. 2*) of length 35 m each and 15 spans in the *Y*-direction of length12 m each. The columns of the structure have a height of 12 m (the height of the building) and a rectangular section of 0.70×0.50 m^2 (*Fig. 3*) with a 40 mm cover. The concrete

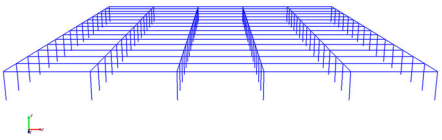

Fig. 1: 3D overview of the building under study

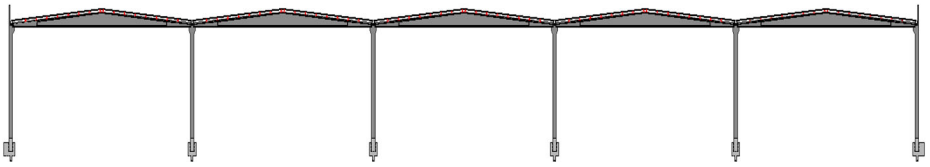

Fig. 2: Principal direction (X) of the framed structure

used is of class C40/50 and the steel of class S500 NR-SD. The longitudinal beams are prestressed with an "I" variable section, with a length of 36 m and a 30 mm cover. The columns are assumed to be fixed to the foundation.

In Europe, the most common type of beam-to-column connection in PRC industrial buildings is the dowel connection. [25] In this system, the beam is mechanically connected to the column by vertical steel dowels. These dowels, usually one or two, protruding from the column's corbel (*Fig. 4*), fit into sleeves left in the edge of the beams, which are later filled with a proper grout. In several cases, a steel or neoprene pad is placed between the column and the beam. These connections do not restrain the rotations between both members, while the transfer of horizontal forces between the beam and column is essentially ensured by friction and dowels (if present). The following sections present a brief description of each of these mechanisms.

Numerical Model Assumptions

As stated before, and considering that, under seismic loads, the damage tends to be concentrated at the bottom of the columns or at the beam-to-column connection, material nonlinearity is considered only in these columns and at the connection level, assuming elastic behavior in both longitudinal and transverse beams.

Reinforced Concrete Elements

The structural behavior of the precast building is simulated along the two main directions with a 3D model using the proprietary computer program OpenSees. [26] In this model, the columns are simulated using nonlinearBeamColumn elements. In terms of materials, the Concrete01 model is used for the concrete, which is based on the Kent–Scott–Park concrete model [27, 28] with degraded linear unloading–reloading stiffness according to Ref. [29] and no strength in tension (see *Fig. 5a*). Regarding the longitudinal reinforcement, the Steel02 model is considered, which is based on the Giuffre–Menegotto–Pinto [30] material model (see *Fig. 5b*).

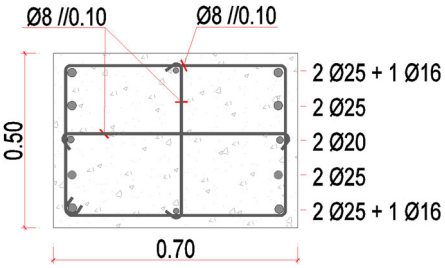

Fig. 3: Column section

As previously mentioned, the beams are modeled as elastic elements in both directions. The "I" beams in the frame direction (*X*-direction) are modeled with elastic elements—once it is assumed that the level of prestress in the beams considerably reduces the damage, the assumption of uncracked sections is sufficiently reliable and followed by other authors. [24] Rectangular beams are also considered in the transverse direction (the *Z*-direction) with linear behavior, and the beam-to-column connection is similar to that in the *X*-direction. Limited damage is expected to the beams either in the longitudinal or transverse direction.

It is recognized that the presence of heavy cladding systems can change the dynamic behavior and the collapse mechanisms [5, 31, 32] of precast buildings. Yet, as noted in Ref. [33], their contribution is mostly relevant during the elastic response phase. Hence, for the present case, the infill walls are assumed to be light with a very low mass, and therefore the effects of cladding panels, and their interaction with the main structure, are not considered in these analyses. Regarding the roof cladding elements, if designed with enough in-plane stiffness and proper connections, these can play an important role in the seismic performance of precast frame structures, [34] ensuring rigid diaphragm behavior. In this case study a light roof cladding system is assumed, and therefore the equivalent dead loads are considered in the model, but the strength and stiffness of the roof system are neglected.

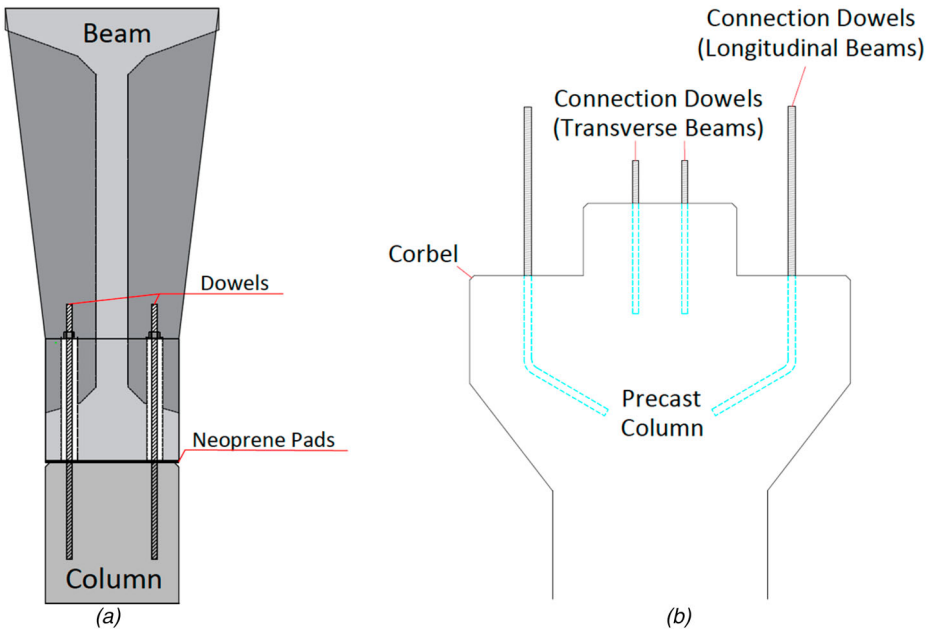

Fig. 4: Scheme of conventional European beam-to-column dowel connection: (a) beam-to-column connection; (b) central column detailing

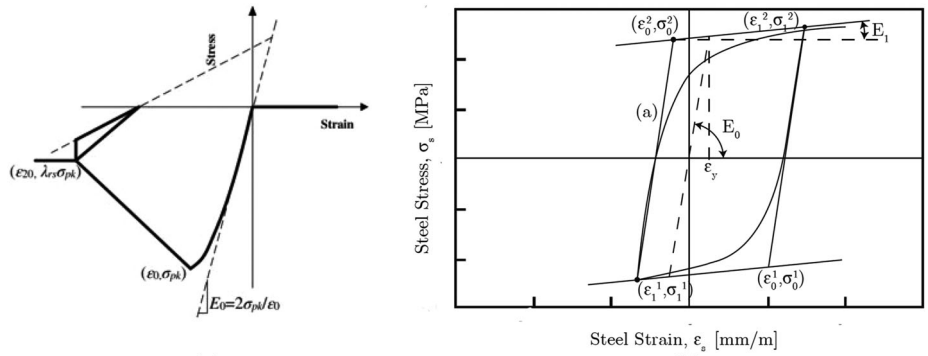

Fig. 5: The material models used and available in OpenSees: (a) parameters of Concrete01; (b) parameters of Steel02

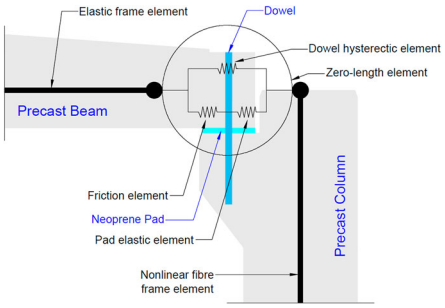

Fig. 6: Numerical model adopted to simulate the behavior of the beam-to-column connections

Parameter	Non-confined concrete		Confined concrete	
Concrete compressive strength at 28 days	*fpc*	48,000 kPa	*fpc_c*	*kpc* × fpc*
Concrete strain at maximum strength	*epsc0*	0.0035	*epsc0_c*	*kpc × epsc0*
Concrete crushing strength	*fpcu*	20% *fpc*	*fpcu_c*	80% *fpc_c*
Concrete strain at crushing strength	*epsU*	5 × *epsc0*	*epsU_c*	5 × *epsc0_c*

Table 1: Parameters to model Concrete 01

Parameter	Steel 02	
Yield strength	F_y	550 × 10^3 kPa
Modulus of steel	E_s	200 × 10^6 kPa
Strain–hardening ratio	b_s	0.005
Parameters to control the transition from elastic to plastic branches	R_0	18
	cR1	0.925
	cR2	0.15

Table 2: Parameters to model Steel 02

The mechanical properties considered for each model are described in *Tables 1, 2*. Second order (P-Delta) effects are considered in all the analyses.

Beam-to-Column Connection

Considering the aim of the present study and the importance of beam-to-column connections in the seismic behavior of PRC structures, [2, 5, 6, 8, 19, 35] the performance of the building is assessed considering different connection properties. These variations are simulated through a macro-element proposed by Sousa et al., [1] which is capable of accurately describing the main mechanisms identified in conventional beam-to-column PRC connections, namely friction between the different elements, steel dowels and the neoprene pad. This macro-element consists of a zero-length element, i.e. the end nodes of the beam and column have the same coordinates, that represent the contribution of the different systems through different springs that are aligned in series or in parallel, depending on the manner these are activated in real structures. The spring arrangement, illustrated in *Fig. 6*, is defined for both horizontal directions, while rotations along the three main directions are released. It is recognized that the macro-model approach has inherent limitations, namely not considering the eccentricity between the line of applied load and the elastomeric bearing, and as such the connection works only in shear.

In addition to the geometric and mechanical properties inherent in the connection, the constitutive models associated with the different springs require the definition of additional calibration parameters, which are described hereinafter. It is noted that these parameters refer to models available in the platform OpenSees, [26] which is the one used to perform the structural analysis of the building. The macro-element used is validated with four experimental tests featuring different geometric, mechanical and loading conditions, showing the capacity to represent the cyclic behavior of the beam-to-column connections, estimating the maximum strength and capturing the main failure mechanisms (dowel rupture and concrete spalling), as well as the strength degradation effects. Additional information regarding the development and calibration of the macro-element model adopted in this study can be found in Ref. [1].

Friction

The simulation of the friction component is carried out incorporating the "VelNormalFrcDep" friction model, into the "flatSliderBearing" zero-length element. This choice allows the computation of the friction coefficient as a function of the installed axial load during the analysis. In this study, the relation between axial load and friction coefficient approaches the behavior observed by Magliulo et al. [36] The representation of the empirical observations is achieved by adopting Eqs. (1) and (2) to define the input parameters of the "VelNormalFrcDep" model, where A_{pad} is the contact area of the pad:

$$a = \frac{0.445}{A_{pad}^{-0.163}} \quad (1)$$

$$n = 0.837 \quad (2)$$

In addition to the incorporation of the

Friction model	
aSlow	Eq. (1)
nSlow	0.837
aFast	Eq. (1)
nFast	0.837
alpha0	0
alpha1	0
alpha2	0
maxMuFat	Eq. (2)
Neoprene pad	
G	1000
Apad (m^2)	0.08
t (m)	0.02
K	Eq. (3)

Table 3: Parameters considered in the definition of the flatSliderBearing element

friction model, consideration of the "flatSliderBearing" element allows the simplification of the connection element, merging the two springs defined in series: the neoprene pad and the friction model. This is achieved by considering the elastic stiffness of the neoprene pad (Eq. 3) as the initial stiffness of the "flatSliderBearing" element:

$$K_{\text{pad}} = \frac{F}{\Delta} = \frac{G \cdot A_{\text{pad}}}{t} \quad (3)$$

In the previous expression, G is the shear modulus of the neoprene, assumed to be equal to 1 MPa according to Fischinger et al., [37] and t is the thickness of the pad. *Table 3* summarizes the parameters considered to model the contribution of the friction and neoprene pad. Considering the limited information in the literature regarding the variation on the friction coefficient with velocity, the parameters alpha0, alpha1 and alpha2 are set to zero, making the model velocity independent.

Dowels

The contribution of the dowels is modeled assuming a trilinear force–displacement relation through the "hysteretic" uniaxial material available in the OpenSees. [26] As illustrated in *Fig. 7*, the backbone curve of this material is defined by six force–displacement pairs.

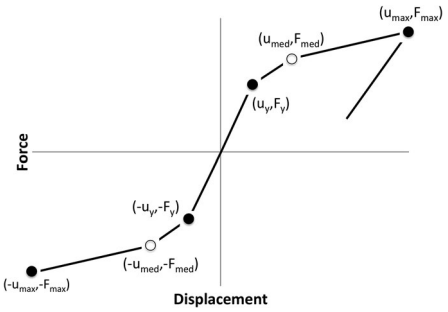

Fig. 7: Generic backbone curve of the model adopted to model the dowel component of the connections

The values corresponding to the yielding (u_y, F_y) and maximum ($u_{\max}$, $F_{\max}$) strength are determined with expressions (4) to (7), following the studies of Refs. [37, 38, 1]:

$$F_y = \frac{K_{\text{conf}} \cdot f_{cc} \cdot d_d (8 \cdot 0.314 \cdot d_d)}{2} \quad (4)$$

$$u_y = \gamma_y \cdot 2 \cdot F_y \frac{(1 - \beta \cdot e)}{(2 \cdot \beta^3 \cdot E_s \cdot I)} \quad (5)$$

$$F_{\max} = K_{\text{conf}} \cdot f_{cc} \cdot d_d \left(a + \frac{2.5 d_d - a}{2} \right) \quad (6)$$

$$u_{\max} = 2 \cdot \tan(\text{rot}_{\max}) \cdot a \quad (7)$$

In the previous equations, K_{conf} is the confinement factor, I is the moment of inertia of the dowel section, E_s is the elastic modulus of the steel used in the dowels, e is the eccentricity of the dowels (assumed to be half the thickness of the neoprene pad), $\text{rot}_{\max}$ is the maximum rotation of the dowels, and β and a are parameters whose expressions can be consulted in the work of Ref. [37]. The confinement factor depends on the concrete strength, size, position and transverse reinforcement around the dowels. In the present study, k_{conf} is considered to equal 2.4, following the findings of Ref. [1]. In well-confined concrete, the failure is local and is characterized by simultaneous yielding of the dowel and crushing of the surrounding concrete; conversely, the failure may be characterized by spalling of the concrete between the dowel and the edge of the columns and/or beams. [1]

In order to account for possible failures due to spalling of the concrete around the dowel, if the ratio between the cover and the diameter of the dowel (D/d_d) is between four and six, the maximum strength ($F_{\max}$) is reduced according to the factor proposed in Ref. [38]:

$$F_{\text{spal}} = \gamma_{spal} \left(0.25 \frac{d_d}{D} - 0.5 \right) F_{\max} \quad (8)$$

In addition to the previous reference values, the force at the intermediate point of the trilinear relation is considered to be equal to the maximum force (expression 9), while the displacement at this point is defined as the yielding displacement plus a fraction of the plastic displacement (expression 10):

$$F_{\text{med}} = F_{\max} \quad (9)$$

$$u_{\text{med}} = u_y + \frac{u_{\max} - u_y}{\gamma_u} \quad (10)$$

In addition to the values defining the backbone curve, the model considers five other parameters to account for the degradation of the dowels resulting from large deformation demand and cyclic degradation. The list of the adopted values in the definition of the dowel model is indicated in *Table 4*, based on the connection properties included in the design project and on the best fit parameters found for the macro-element used to represent the beam-to-column connection, which is validated against experimental tests. [1]

Static Loads and Seismic Action

For the numerical analyses, constant vertical loads distributed on beams are considered to simulate the dead load of the self-weight of the roof and PRC elements, and the corresponding quasi-permanent value of the live loads, giving a total value of 0.65 kN/m^2. The mass of the structure is also assumed to be distributed at beam level. The 2D and 3D models are subjected to incremental dynamic analysis (IDA). A total of 20 ground motion records are selected from real seismic events according to the method due to Ref. [39]. The ground-motions are divided into 2 groups of 10 records, whose average spectrum fits the Eurocode 8 target spectrum for Type 1 and Type 2 for Lisbon and soil type A, as illustrated in *Fig. 8*.

Connection properties	
$E_{S,dowel}$ (MPa)	200,000
$F_{Y,dowel}$ (MPa)	550
$F_{U,dowel}/F_{Y,dowel}$	1.2
Fc (MPa)	48
Number dowels, *P*	2
d_P (mm)	24
a_P	29.4
β_P	0.025
$rot_{max,P}$	0.4
$dd_{P,X}$ (mm)	150
$dd_{P,Y}$ (mm)	140
Number dowels, S	2
d_S (mm)	20
a_S	24.5
β_S	0.030
$rot_{max,S}$	0.4
$dd_{S,X}$ (mm)	80
$dd_{s,Y}$ (mm)	150
Numerical model properties	
F_y, F_m, F_u, u_y, u_m, u_u	Expressions 4–10
K_{Conf}	2.4
γ_y	3.5
γ_{Spal}	1.1
γ_u	6
pinchX	0.5
pinchY	0.5
damage1	0
damage2	0.06
beta	0.01

Table 4: Parameters considered in the definition of the hysteretic model

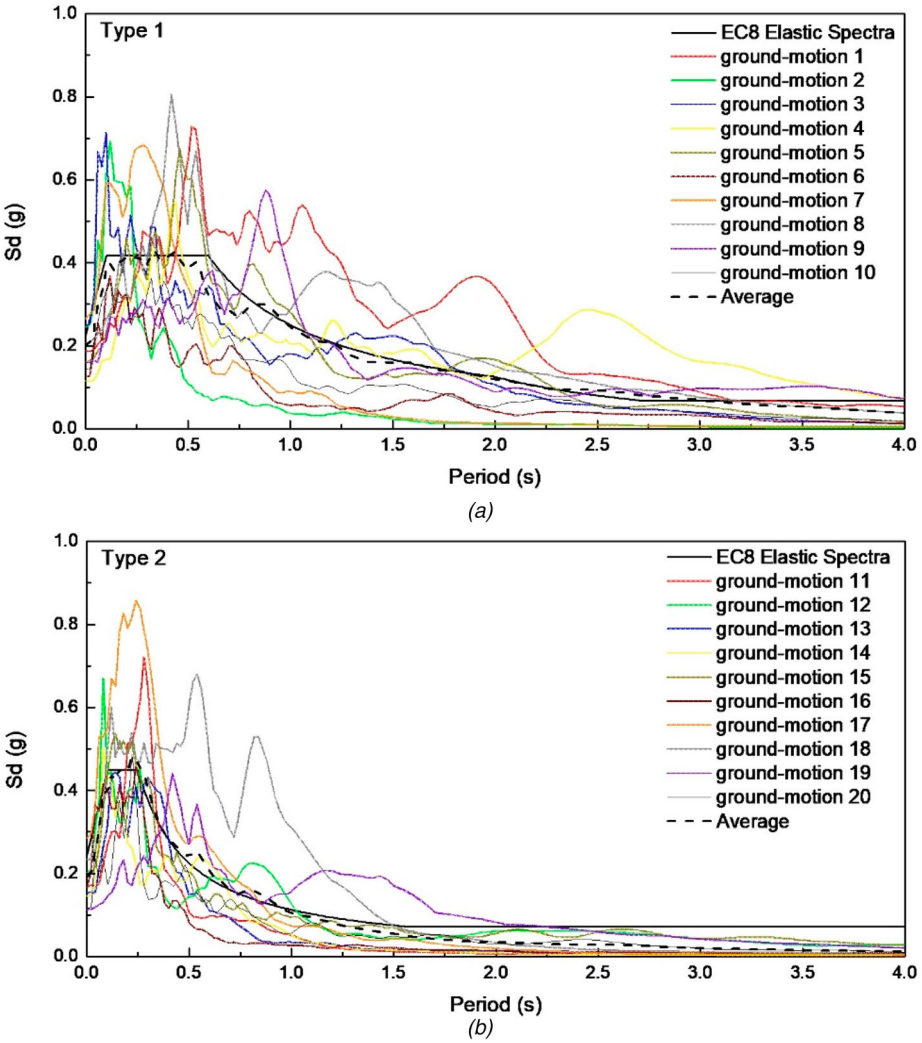

Fig. 8: Elastic spectrum of the ground motions selected: (a) Type 1; (b) Type 2

Parametric Study

To understand the seismic performance of the structure, a parametric study is designed. Initially, a comparison is performed between the 2D and 3D models in the *X*-direction. After that, the impact of the two different earthquake loads is analyzed using the 3D model. Then, also using the 3D model, several cases are considered with the aim of better understanding the impact that certain parameters have on the response of the building being studied. The parameters considered are the height of the column, the type of connection (diameter of the dowels, neoprene pad and friction) and the level of axial load. All the different cases considered are detailed in *Table 5*. Each case is named according to the properties considered in the model; for example,

ID	Properties					
	Height (m)	Axial load (kN)	Number/Diameter of dowels (mm)		Friction	Neoprene pad (mm)
			X-*direction*	Y-*direction*		
PC	**12**	**477.4**	**Pinned connection**			
DFNC	**12**	**477.4**	**2 Ø24**	**2 Ø20**	**Yes**	**20**
DC	**12**	**477.4**	**2 Ø24**	**2 Ø20**	**NC**	**NC**
FNC	**12**	**477.4**	**NC**	**NC**	**Yes**	**20**
LDFNC	12	727.4	2 Ø24	2 Ø20	Yes	20
LFNC	12	727.4	NC	NC	Yes	20
DFNC6	6	477.4	2 Ø24	2 Ø20	Yes	20
D2FNC6	6	477.4	2 Ø16	2 Ø16	Yes	20
NC: Not Considered in the model.						

Table 5: List of the properties adopted in the different models

the case "DFNC" corresponds to a Dowel, Friction and Neoprene Connection considered in the model. In the same way, the case "DC" corresponds to a Dowel Connection and the case "FNC" corresponds to a Friction and Neoprene Connection considered in the model. The case "LDFNC" is the same as case DFNC but with a higher axial load, the case "DFNC6" is the same as case DFNC but with a lower height, and case "D2FNC6" is the same as case DFNC6 but with dowels of lower diameter.

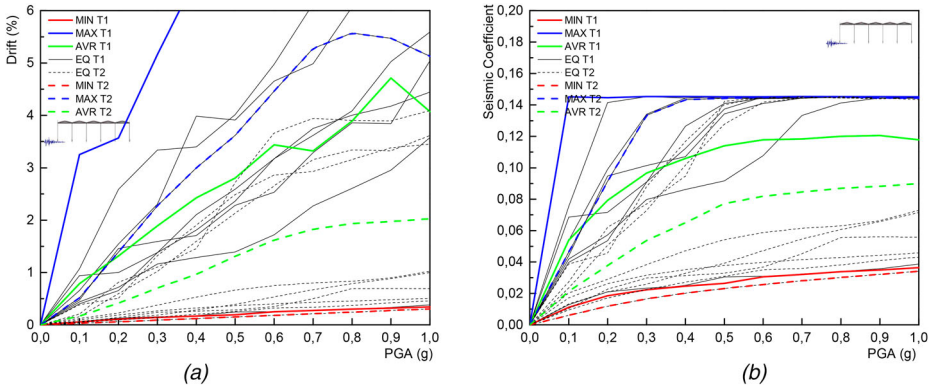

Fig. 9: 2D model (12 m) with pinned connections for earthquake Types 1 and 2: (a) maximum drift comparison; (b) seismic coefficient comparison

Discussion of the Results

This section discusses the results obtained for the prototype building under study considering the different changes considered in the parametric study. The results are discussed in terms of maximum inter-story drift, seismic coefficient and relative displacement at the connection level between the column and the beam. The seismic coefficient is defined by the ratio of the base shear to the total weight of the structure. The main aim of the analysis is to identify the main properties that influence the seismic behavior of a precast industrial building. Previous research on PRC framed buildings showed a large dispersion in the drift values, ranging from 3% to 8%, [7] highlighting the current difficulties in the definition of appropriate limit states for PRC structures. In the present study, a maximum drift of 6% is considered for the sake of comparison between the different models.

2D assessment of the Earthquake Type

The aim of the first analysis is to compare the effect of Type 1 and Type 2 earthquakes in the 2D models. *Figure 9* presents the results in terms of maximum drifts and seismic coefficient. The results show that, for similar peak ground accelerations (PGAs), the drift and seismic coefficient are higher when the structure is subjected to earthquakes representative of the Type 1 spectrum. This effect is related to the longer duration and the larger spectral ordinates associated with Type 1 earthquake records. As noted in the following sections, the first frequency of the structure is 0.66 Hz (T1 = 1.5 s), which corresponds to higher spectral accelerations for Type 1 earthquakes when compared with those associated with Type 2 records. This effect can be observed in *Fig. 8* where, for the first mode (T1 = 1.5 s), the elastic spectra associated with Type 2 (approximately 0.1 g) is significantly lower than those characteristic of Type 1 (approximately 0.2 g) spectra. For this reason, the seismic demand associated with Type 2 seismic action is substantially lower for the structure analyzed. Considering this and from now on, for the sake of simplicity, the analyses presented hereinafter consider only the results obtained for Type 1 earthquakes.

The 2D and 3D Models

The 2D and 3D models with pinned connections are analyzed to compare behavior between the 2D and 3D models in the *X*-direction and to compare both directions in the 3D model. This type of comparison can show which models should be developed to study certain aspects of the structure. In fact, several authors have already highlighted the importance of considering a 3D analysis in precast industrial buildings. [9, 19] This section presents a comparative analysis of the maximum inter-story drifts and seismic coefficients of the 2D and 3D models. *Figure 10* shows that the drifts and seismic coefficients are similar for the *X*-direction; the main differences are observed for higher levels of PGA and for large incursions into the nonlinear behavior. The main advantages of considering the 3D model are related to the study of the orthogonal direction and the consideration of three components of the earthquake records, accounting for directionality effects, eventual plan irregularities, either present or introduced by the panels, among other aspects. In particular cases, it can be considered that a simplified model (the 2D model) can perhaps be an acceptable and reliable method to represent a more complex structure (the 3D model) and to study some aspects of the complex structure. Similar findings have already been observed by Beilic et al. [24] In *Fig. 11*, a comparison between the *X*- and *Y*-directions can be observed and, for the case under study, for the same PGA, the drift demand is similar, especially for

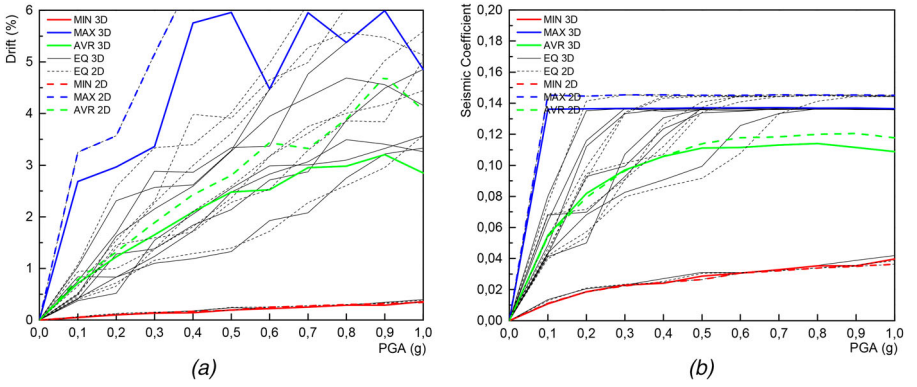

Fig. 10: 2D and 3D models (12 m) with pinned connections for Type 1 earthquake: (a) maximum drift comparison; (b) seismic coefficient comparison

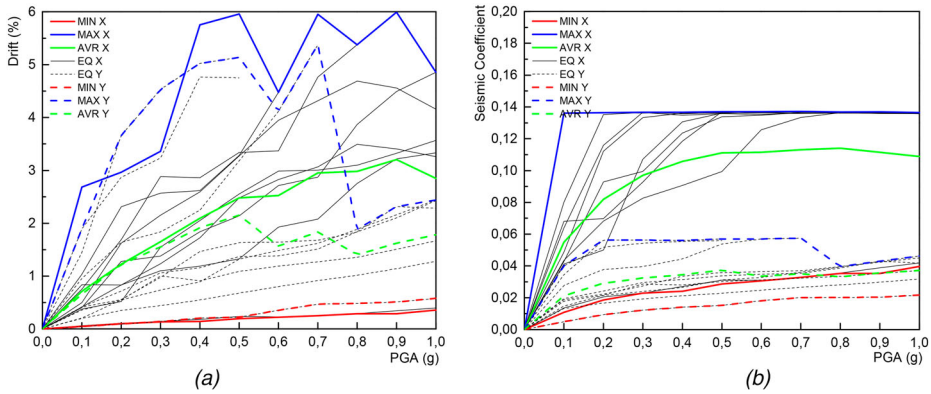

Fig. 11: 3D model (12 m) with pinned connections for Type 1 earthquake in the X- and Y-directions: (a) maximum drift comparison; (b) seismic coefficient comparison

	Height			
	6 m		12 m	
Connection	**Frequency (Hz)**		**Frequency (Hz)**	
DFNC	f_1	1.26	f_1	0.44
	f_2	1.85	f_2	0.65

Table 6: Frequency comparison between the models with 6 and 12 m and DFNC connection

PGAs lower than 0.5 g. But the differences in the seismic coefficient between the two directions are significant. Owing to the use of the structural solution, the capacity of the buildings is significantly higher in the *X*-direction.

Effect of Story Height

The height of the columns of precast buildings can vary significantly, but usually range between 6 and 12 m. To assess the effect of story height, the 12 m column height of the reference building (DFNC) was reduced to 6 m in the new model (DFNC6). The first relevant outcome of this comparison regards modification of the dynamic properties of the buildings. As expected, *Table 6* shows that the main natural frequencies of the 6 m high structure are almost three times higher than the frequencies of the 12 m high structure. By reducing the height of the building, there is an increase in stiffness that leads to higher frequencies of the structure and possible modifications in the seismic response as a function of different frequency content of ground motions.[40, 41]

In addition, the decrease in the column's height leads to a reduction in the column's horizontal displacement and drift capacity. On the other hand, the lateral capacity, and hence the seismic coefficient, increases significantly, as illustrated in *Fig. 12*.

Concerning the behavior of the connection, it is interesting to note that the sliding of the connection increases in the DFNC6 model. This effect highlights the need to adjust the connection properties as a function of the column's capacity. With a reduction in the column's height (and keeping the connection properties unchanged) the shear forces on the column increase, leading to an increase in the connection force and consequently the lateral deformation. In other words, in order to exhibit an adequate seismic behavior, the connection strength should be equal to at least the column's maximum horizontal strength (*Fig. 13*).

Contribution of the Connection to the Global Behavior

One of the main aims of the present study is to assess the effects of the connection on the global behavior of the building under study. The changes are presented in *Table 5* and the results obtained are discussed next. *Table 7* presents the 1st and 2nd frequencies of the different 3D structures with different connections and characteristics. The 3D models with pinned connections (PCs) and DFNC connections have the same frequencies. This situation shows that, for this model, when analyzing the frequencies, considering a detailed connection with dowel, neoprene and friction is the same as considering a pinned connection.

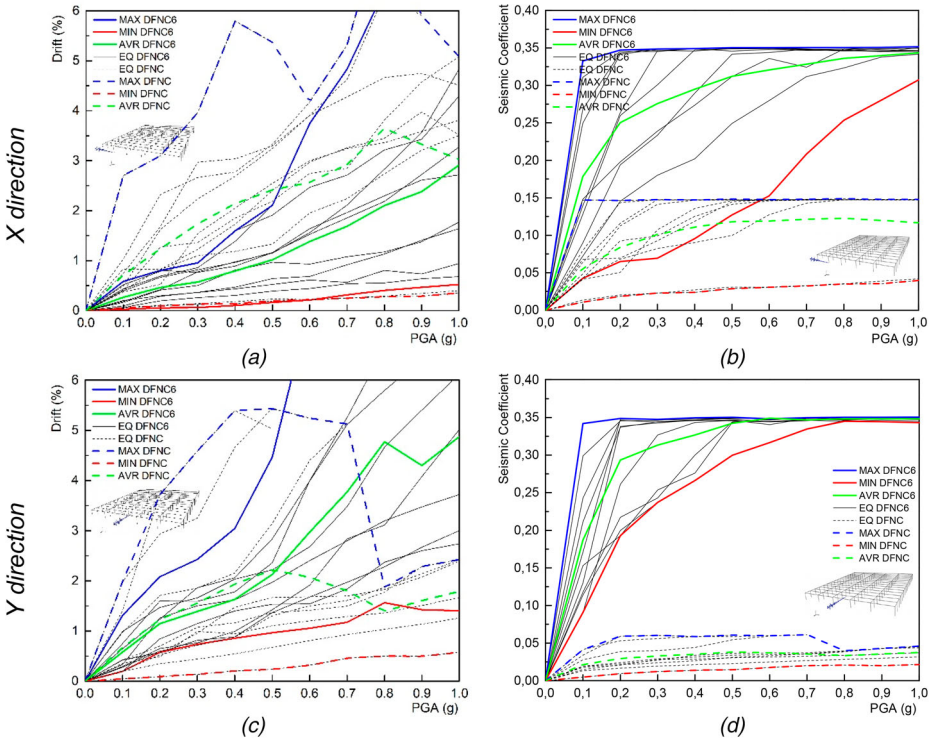

Fig. 12: DFNC6 (6 m) and DFNC (12 m) 3D models for Type 1 earthquake in the X- and Y-directions: (a) maximum drift in the X-direction; (b) seismic coefficient in the X-direction; (c) maximum drift in the Y-direction; (d) seismic coefficient in the Y-direction

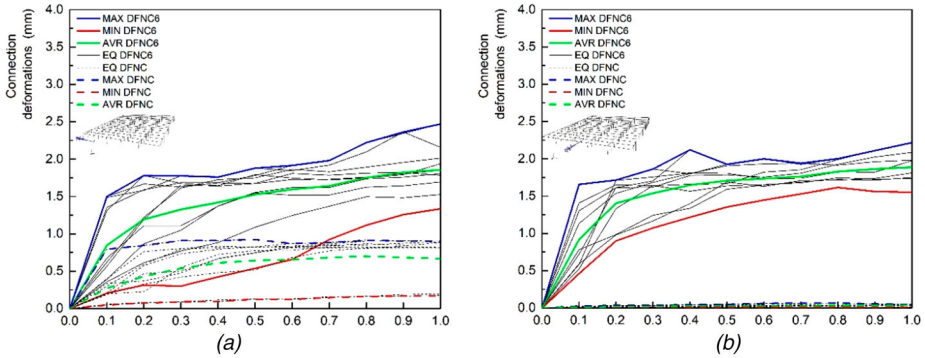

Fig. 13: Connection sliding in DFNC6 (6 m) and DFNC (12 m) 3D models: (a) X-direction; (b) Y-direction

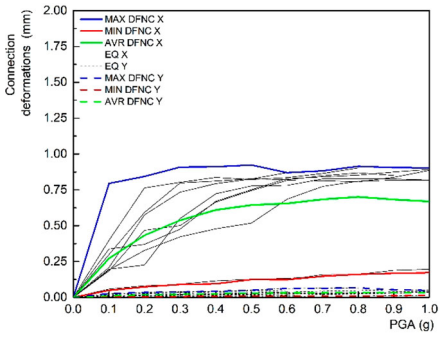

Fig. 15: Connection sliding in the X- and Y-directions in the DFNC model

Model	Frequency	
	f1	f2
PC	0.44	0.65
DFNC	0.44	0.65
DC	0.44	0.65
FNC	0.44	0.48
LDFNC	0.36	0.53
LFNC	0.36	0.38
DFNC6	1.25	1.53
D2FNC6	1.24	1.48

Table 7: Frequency comparison between the models with different connections and characteristics

The 3D models with DFNC and DC connections have the same frequencies, which shows the very low impact of the neoprene and friction on the structure's frequency. On the other hand, the 3D models with DFNC and FNC connections have different contributions to the global stiffness of the structure, which shows that the dowels may have a significant impact on structure's behavior in terms of strength, as expected, but also on the global stiffness. Comparing the DFNC and LDFNC models, where the only difference between the models is the higher mass applied in the LDFNC model, it is possible to see that the LDFNC model has a lower frequency. The LFNC model can be compared with the FNC and the LDFNC models. In both comparisons, the LFNC model is the one with lower frequencies, which shows, as previously observed, that an increase in the mass and a reduction of the dowels lead to lower frequencies. The conclusions regarding the comparison between the DFNC and DFNC6 models are the same as presented earlier when discussing the results in *Table 6*. Finally, comparing the DFNC6 model with the D2FNC6 model, where the only difference is the lower diameter of the dowels in the D2FNC6 model, it is possible to see that the D2FNC6 model presents a slightly lower frequency when compared with the DFNC6 model, which shows that a lower diameter of the dowel leads to a lower frequency of the structure. This aspect follows the same idea as the comparison between the DFNC and FNC models, where the absence of dowels leads to a lower frequency of the structure.

DFNC Connection and Pinned Connection

This section compares the DFNC model with the PC model to find the difference between considering a model with a dowel, friction and neoprene connection, and a model with pinned connections, as usually considered in common design practice. *Figure 14* presents the drifts and seismic coefficients for the DFNC and PC models in both directions. The differences between the DFNC and PC models are very low, indicating that, in cases where the connection is adequately designed, i.e. the connection is capacity protected with respect to the level of forces expected in the

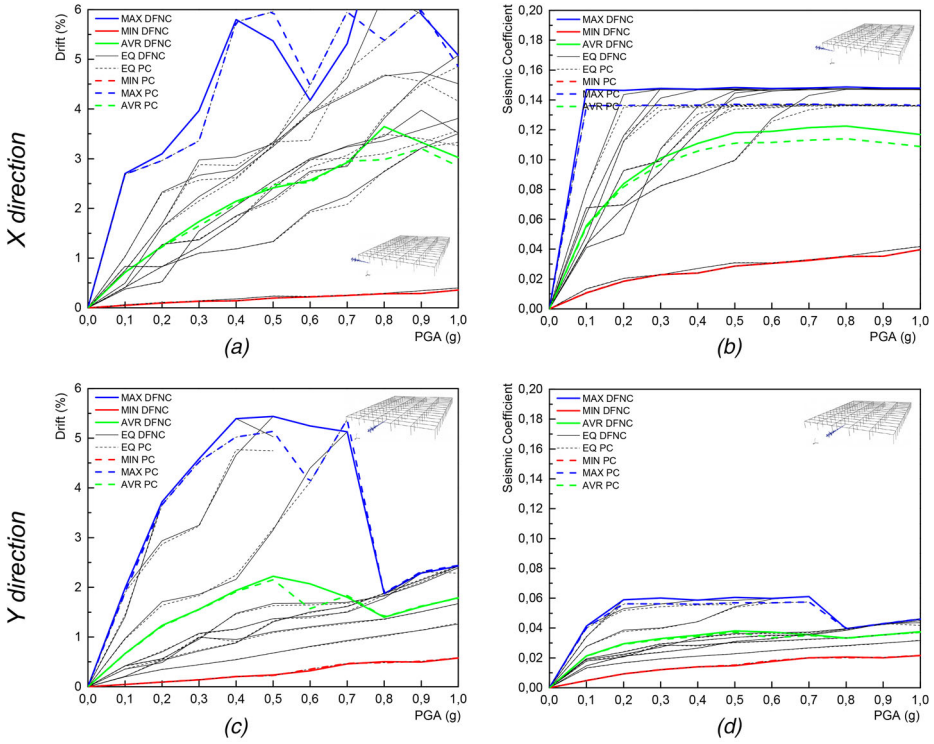

Fig. 14: 3D model (12 m) with pinned and DFNC connections for Type 1 earthquake in the X- and Y-directions: (a) drift comparison in the X-direction; (b) seismic coefficient comparison in the X-direction; (c) drift comparison in the Y-direction; (d) seismic coefficient comparison for Y-direction

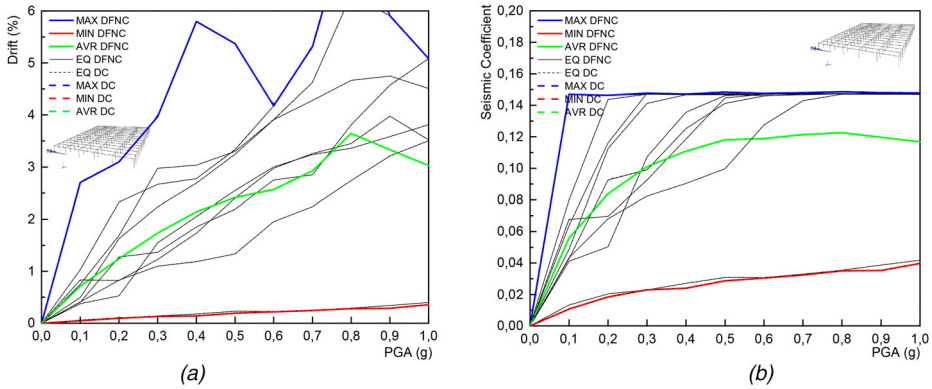

Fig. 16: 3D model (12 m) with DC and DFNC connections for Type 1 earthquake in the X-direction: (a) drift comparison; (b) seismic coefficient comparison

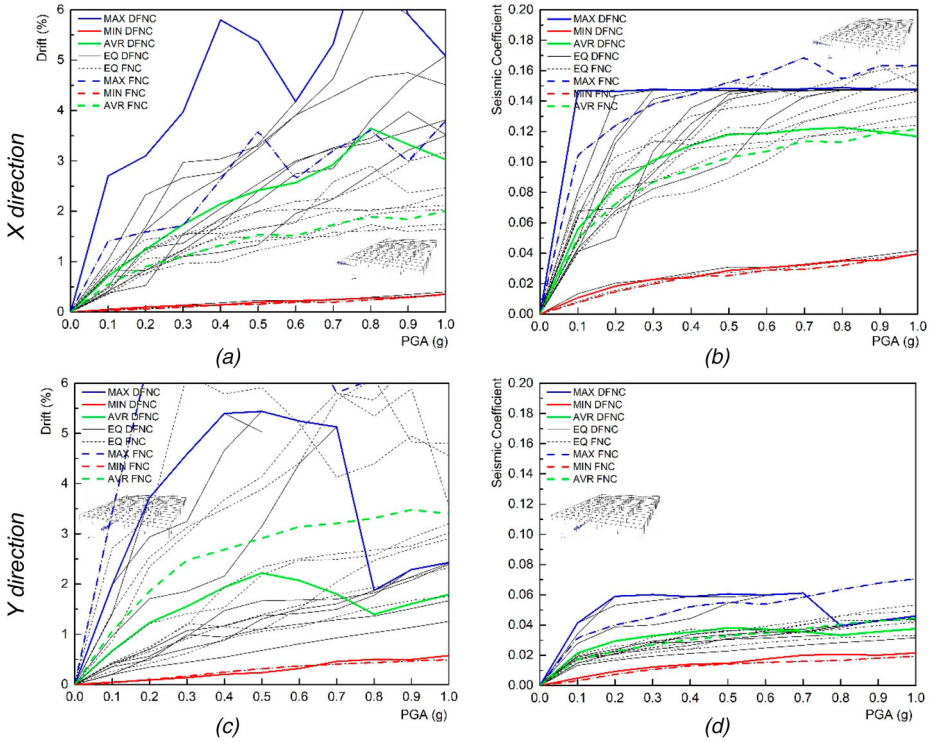

Fig. 17: 3D model (12 m) with DFNC and FNC connections and for Type 1 earthquake in the X- and Y-directions: (a) drift comparison in the X-direction; (b) seismic coefficient comparison in the X-direction; (c) drift comparison in the Y-direction; (d) seismic coefficient comparison in the Y-direction

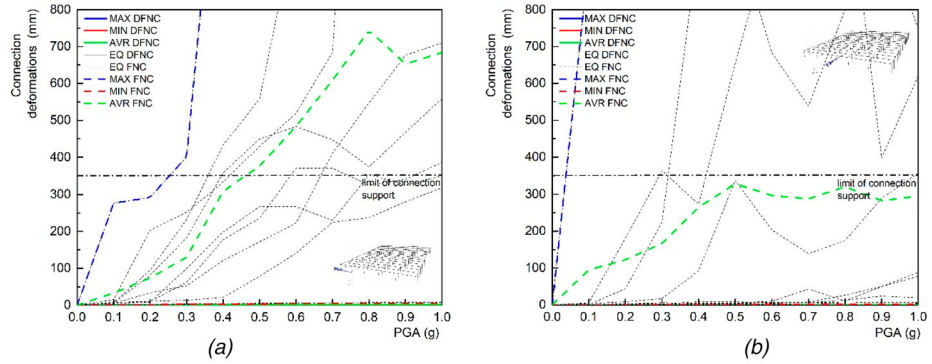

Fig. 18: Connection sliding in 3D model (12 m) with DFNC and FNC connections for Type 1 earthquake: (a) X-direction; (b) Y-direction

adjacent columns, the seismic behavior of the building can be modeled with acceptable accuracy using simple pinned connection models. The observation that the sliding of the connection in the *X*-direction is considerably higher than that in the *Y*-direction is related to the higher shear forces developed along the *X*-direction, which correspond to the columns stronger direction (*Fig. 15*).

Effect of the Neoprene and Friction

This section discusses comparisons of the drift and seismic coefficient of 3D models with DC and DFNC connections, to evaluate the effect of a connection with dowel only with that of a connection with dowel, friction and neoprene. For the building under study, this effect seems not to play a significant role. *Figure 16* shows that the influence of the friction and neoprene is low in terms of the drift and seismic coefficient of the structure. In fact, previous studies [1] pointed to a contribution of the friction and neoprene of around 25% of the global connection response. Such values are not observed in this case because the columns are significantly more flexible than connections with dowels, even if the friction and neoprene are neglected, and therefore the horizontal response of the building is governed by the flexibility of the columns.

Effect of the Dowels

This section presents a comparative analysis of the 3D models with FNC and DFNC connections. *Figure 17* shows a significant difference between considering FNC and DFNC connections, which highlights the importance of the dowels in the overall seismic behavior of the structure. For the same level of PGA, the columns in the model without dowel presents a lower drift demand when compared with the model with dowels. On the other hand, DFNC connections have higher seismic coefficients when compared with the FNC connections (see *Figs. 17b*, *17d*) due to the connection sliding that in the models without dowel are much higher than those with dowels (*Fig. 18*). The previous observations show that, in the model without dowel, the deformations are essentially concentrated in the connection. Assuming a limit for connection maximum sliding of 350 mm based on

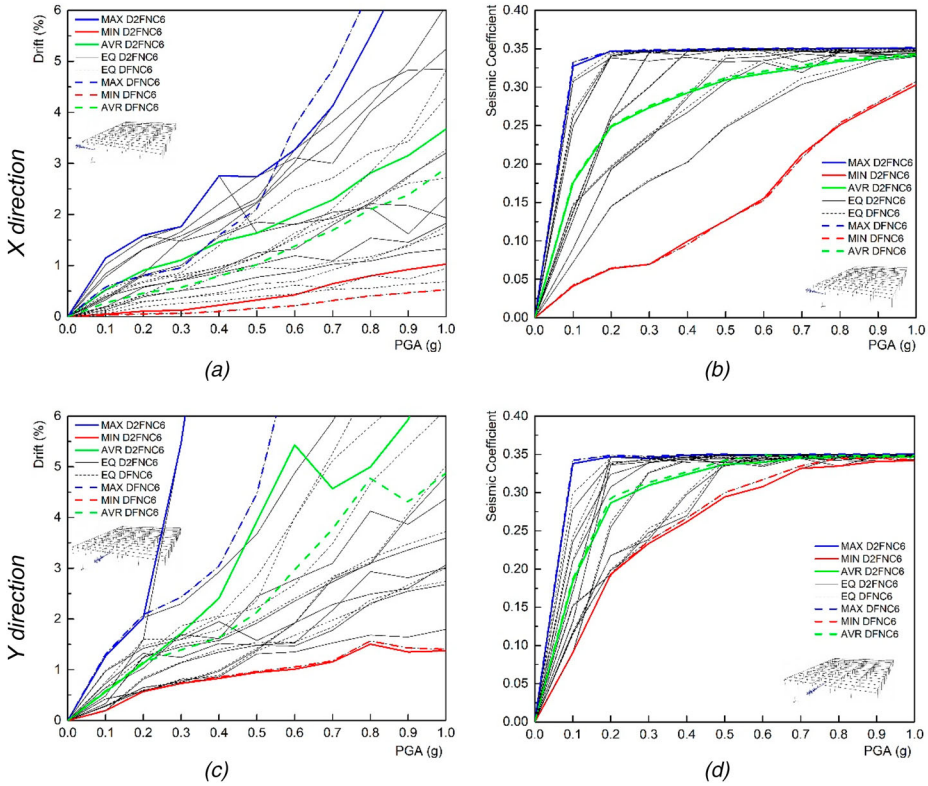

Fig. 19: D2FNC6 and DFNC6 3D models (6 m) for Type 1 earthquake in the X- and Y-directions: (a) drift comparison in the X-direction; (b) seismic coefficient comparison in the X-direction; (c) drift comparison in the Y-direction; (d) seismic coefficient comparison in the Y-direction

typical geometric properties of the beams support, [42] it is possible to see that, for PGA higher than 0.45 g, the connection fails for the average of the analyses.

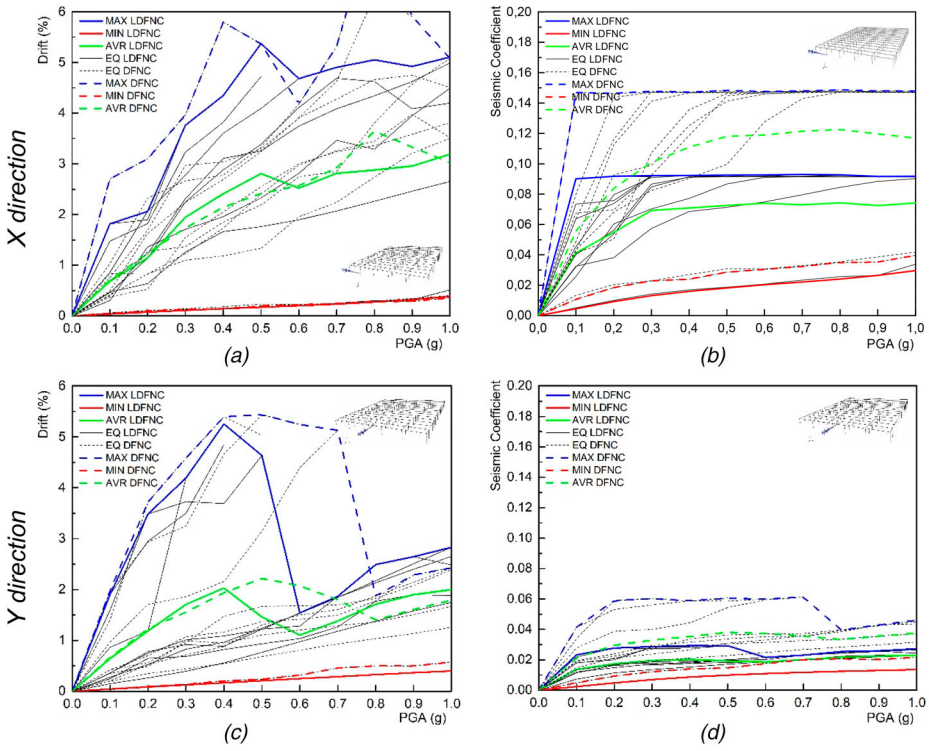

Fig. 20: LDFNC and DFNC 3D models (12 m) for Type 1 earthquake in the X- and Y-directions: (a) drift comparison in the X-direction; (b) seismic coefficient comparison in the X-direction; (c) drift comparison in the Y-direction; (d) seismic coefficient comparison in the Y-direction

The results observed are in line with the damage observed after past seismic events such as the Emilia earthquake of 20 and 29 May 2012. In fact, the damage observed in the connections occurs essentially in buildings without dowels. In these cases, the horizontal strength at the connection level is ensured essentially by friction and hence its capacity to sustain horizontal loads is severely compromised. This observation highlights the need to consider detailed connections models, capable of simulate the different strength mechanisms at the connections, to conduct reliable seismic assessment of existing buildings, especially those built without considering steel dowels.

Influence of the Dowel Diameter

This section compares models having connections with dowels of different diameter—the DFNC6 connection has 2 Ø24 in the *X*-direction and 2 Ø20 in the *Y*-direction, while the D2FNC6 connection has 2 Ø16 in both principal directions.

Figure 19 shows that the seismic coefficient remains essentially unchanged regardless of the diameter of the dowels considered, indicating that the connection strength remains higher than the maximum capacity of the columns, despite the reduction in the dowels' diameter. In terms of drifts, the results of the DFNC6 model are slightly larger as a consequence of a reduction in the connection stiffness of the D2FNC6 model when compared with the DFNC6 model. Despite being limited to the structural properties admitted in the case study presented in this paper, the results obtained indicate that the presence of dowels, even of small diameter, substantially increases the connection strength, avoiding undesired brittle connection failures.

Effect of Vertical Roof Load

This section analyzes the effect of the vertical roof load in models with dowels (DFNC) and without dowels (FNC). The vertical roof loads and corresponding mass are applied to the extremities of beams oriented along the *X*-direction, introducing modifications to the frequency of the structure, the level of axial force in the columns, and the friction strength at the beam–column interface. In the DFNC and FNC models, a load of 477.4 kN is applied, while in the

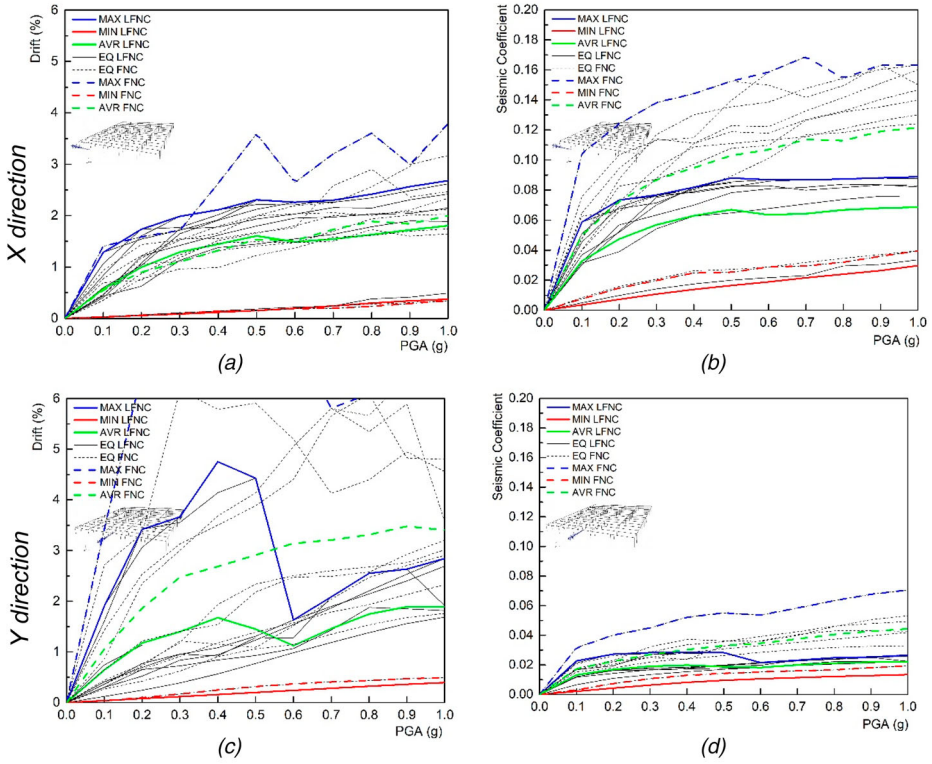

Fig. 21: LFNC and FNC 3D models (12 m) for Type 1 earthquake in the X- and Y-directions: (a) drift comparison in the X-direction; (b) seismic coefficient comparison in the X-direction; (c) drift comparison in the Y-direction; (d) seismic coefficient comparison in the Y-direction

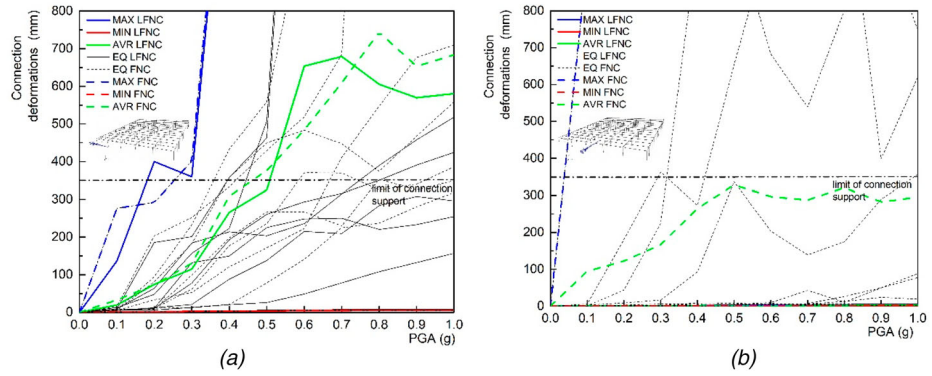

Fig. 22: Connection sliding in the LFNC and FNC models: (a) X-direction; (b) Y-direction

LDFNC and LFNC models the load applied is 727.4 kN.

The results obtained show that the consideration of a higher axial load introduces important modifications to the seismic behavior of the building. A first and direct consequence concerns a considerable reduction in the seismic coefficient due to the increment in the self-weight of the building. In addition, modifications to the dynamic properties of the buildings (an increase in the fundamental period of vibration) will naturally change (generally reduce) the seismic demand. On the other hand, an increase in the axial load at the connection level will result in an increment in the friction strength, and hence in the overall connection strength (*Figs. 20, 21*). This latter observation is particularly relevant along the *Y*-direction, where this increment in strength drastically reduces sliding of the connection (*Fig. 22*).

Conclusions

This paper presents a parametric study carried out through a series of nonlinear dynamic analyses on 2D and 3D PRC building models aiming to evaluate the importance of different sensitivity parameters, namely earthquake type, story height, and contribution of the different beam-to-column connection mechanisms, to the seismic behavior of precast reinforced concrete buildings. For this purpose, the properties of the numerical model developed are defined to mimic common industrial buildings with this typology. For this reason, it is believed that the discussion of the results obtained in this study are not necessarily limited to the case study considered, and that it is possible to extract conclusions that are valid for the generality of this type of building.

PRC buildings are generally flexible structures when compared with conventional RC buildings. For this reason, these buildings tend to be more sensitive to ground motion from distant epicenters, which tend to present larger spectral accelerations for longer periods of vibration (commonly designated as seismic action Type I, according with EC8). In regular buildings, consideration of a simplified 2D model can be acceptable. On the other hand, the consideration of 3D modeling is recommended when in the presence of plan irregularities such as those introduced by cladding panels.

Connection sliding (i.e. relative deformation between the column and the beam) may be affected by several parameters, and the first is related to story height: lower buildings usually lead to an increase in the shear forces in the columns and also introduce higher demands on the connections.

Associated with the previous consideration, it is also observed that buildings having lower height tend to experience larger seismic loads, both in terms of forces and displacements, as a result of a decrease in their natural period of vibration and consequent approximation to the frequency content of typical ground motions.

Regarding the seismic behavior of beam-to-column connections, from a general point of view, the results show the importance of these elements to the seismic behavior of the entire structure. In the presence of adequately designed dowels, small deformations are expected at the connections level, and therefore the response of such structures is

controlled by the properties of the columns. For these cases, the consideration of a simple pinned connection appears to be an efficient and accurate numerical approach.

On the other hand, in the absence of dowels, or in cases where these are not properly designed, a concentration of damage is expected to occur at the connection level, whilst the columns remain essentially undeformed, which is in line with the damage observed in field observations after recent earthquakes.

For intermediate cases, i.e. beam-to-column connections featuring conventional diameter dowels, the explicit consideration of the connection properties through a reliable numerical model is advocated in order to estimate the actual capacity of the connection, especially in terms of deformation, in order to avoid local damage or even the collapse of the beams.

Funding

This work was financially supported by Project POCI-01-0145-FEDER-028439 – "SeismisPRECAST Seismic performance Assessment of existing Precast Industrial buildings and development of Innovative Retrofitting sustainable solutions" funded by FEDER funds through COMPETE2020 - Programa Operacional Competitividade e Internacionalização (POCI) and by national funds (PIDDAC) through FCT/MCTES. This work was also supported by the Foundation for Science and Technology (FCT) - Aveiro Research Centre for Risks and Sustainability in Construction (RISCO), Universidade de Aveiro, Portugal [FCT/UIDB/ECI/04450/2020]. The second and third author acknowledged to FCT - Fundação para a Ciência e a Tecnologia namely through the PhD grant with reference SFRH/BD/148582/2019 and SFRH/BD/139723/2018.v

ORCID

Hugo Rodrigues http://orcid.org/0000-0003-1373-4540
Hugo Vitorino http://orcid.org/0000-0002-6213-2119
Nádia Batalha http://orcid.org/0000-0002-6313-7333
Romain Sousa http://orcid.org/0000-0003-1213-8376
Paulo Fernandes http://orcid.org/0000-0002-5644-8889
Humberto Varum http://orcid.org/0000-0003-0215-8701

References

[1] Sousa R, Batalha N, Rodrigues H. Numerical simulation of beam-to-column connections in precast reinforced concrete buildings using fibre-based frame models. *Eng Struct*. 2020; 203: 109845. doi:10.1016/j.engstruct.2019.109845

[2] Belleri A, Brunesi E, Nascimbene R, Pagani M, Riva P. Seismic performance of precast industrial facilities following major earthquakes in the Italian territory. *J Perform Constr Facil*. 2014; 29 (5): 1–31.

[3] Sezen H, Whittaker A. Seismic performance of industrial facilities affected by the 1999 Turkey earthquake. *J Perform Constr Facil*. 2006; 20: 28–36.

[4] Liberatore L, Sorrentino L, Liberatore D, Decanini L. Failure of industrial structures induced by the Emilia (Italy) 2012 earthquakes. *Eng Fail Anal*. 2013; 34: 629–647. doi:10.1016/j.engfailanal.2013.02.009

[5] Magliulo G, Ercolino M, Petrone C, Coppola O, Manfredi G. The Emilia earthquake: seismic performance of precast reinforced concrete buildings. *Earthq Spectra*. 2014; 30(2): 891–912. doi:10.1193/091012EQS285M

[6] Batalha N, Rodrigues H, Varum H. Seismic performance of RC precast industrial buildings — learning with the past earthquakes. *Innov Infrastruct Solut*. 2019: 1–13. doi:10.1007/s41062-018-0191-y

[7] Sousa R, Batalha N, Silva V, Rodrigues H. Seismic fragility functions for Portuguese RC precast buildings. *Bull Earthq Eng*. 2020. doi:10.1007/s10518-020-01007-7

[8] Bournas D, Negro P, Taucer FF. Performance of industrial buildings during the Emilia earthquakes in northern Italy and recommendations for their strengthening. *Bull Earthq Eng*. 2014; 12(5): 2383–2404. doi:10.1007/s10518-013-9466-z

[9] Demartino C, Vanzi I, Monti G, Sulpizio C. Precast industrial buildings in Southern Europe: loss of support at frictional beam-to-column connections under seismic actions. *Bull Earthq Eng*. 2018; 16(1): 259–294. doi:10.1007/s10518-017-0196-5

[10] Cornali F, Belleri A, Marini A, Riva P. Influence of modelling assumptions in the expected loss evaluation of a precast industrial building. *Procedia Eng*. 2017; 199: 3510–3515. doi:10.1016/j.proeng.2017.09.499

[11] Romão X, et al. Field observations and interpretation of the structural performance of constructions after the 11 May 2011 Lorca earthquake. *Eng Fail Anal*. 2013; 34: 670–692. doi:10.1016/j.engfailanal.2013.01.040

[12] Nascimbene R. Numerical model of a reinforced concrete building: earthquake analysis and experimental validation. *Period Polytech Civ Eng*. 2015; 59(4): 521–530.

[13] Oinam Romanbabu RM, Kumar A, Sahoo Dipti R. Cyclic performance of steel fiber-reinforced concrete exterior beam-column joints. *Earthquakes Struct*. 2019; 16(5): 533–546. doi:10.12989/EAS.2019.16.5.533

[14] Oinam RM, Sahoo DR, Sindhu R. Cyclic response of non-ductile RC frame with steel fibers at beam-column joints and plastic hinge regions. *J Earthq Eng*. 2014; 18 (6): 908–928. doi:10.1080/13632469.2014.916239

[15] Rodrigues H, Romão X, Andrade-Campos A, Varum H, Arêde A, Costa AG. Simplified hysteretic model for the representation of the biaxial bending response of RC columns. *Eng Struct*. 2012; 44. doi:10.1016/j.engstruct.2012.05.050

[16] Bianchi F, Nascimbene R, Pavese A. Experimental vs. numerical simulations: seismic response of a half scale three-storey infilled RC building strengthened using FRP retrofit. *Open Civ Eng J*. 2017: 1158–1169. doi:10.2174/1874149501711011158

[17] Clementi F, Scalbi A, Lenci S. Seismic performance of precast reinforced concrete buildings with dowel pin connections. *J Build Eng*. 2016; 7: 224–238. doi:10.1016/j.jobe.2016.06.013

[18] Beilic D, Casotto C, Nascimbene R, Cicola D, Rodrigues D. Seismic fragility curves of single storey RC precast structures by comparing different Italian codes seismic fragility curves of single storey RC precast structures by comparing different Italian codes. *Earthq Struct*. 2017; January. doi:10.12989/eas.2017.12.3.359

[19] Casotto C, Silva V, Crowley H, Nascimbene R, Pinho R. Seismic fragility of Italian RC precast industrial structures. *Eng Struct*. 2015; 94: 122–136. doi:10.1016/j.engstruct.2015.02.034

[20] Magliulo G, Fabbrocino G, Manfredi G. Seismic assessment of existing precast industrial buildings using static and dynamic nonlinear analyses. *Eng Struct*. 2008; 30(9): 2580–2588. doi:10.1016/j.engstruct.2008.02.003

[21] Elsanadedy HM, Almusallam TH, Alsalloum YA, Abbas H. Investigation of precast RC beam-column assemblies under column-loss scenario. *Constr Build Mater*. 2017; 142: 552–571. doi:10.1016/j.conbuildmat.2017.03.120

[22] Feng D, Wu G, Lu Y. Finite element modelling approach for precast reinforced concrete beam-to-column connections under cyclic loading. *Eng Struct*. 2018; 174(May): 49–66. doi:10.1016/j.engstruct.2018.07.055

[23] Kataoka M, Ferreira M, Debs A. Nonlinear FE analysis of slab-beam-column connection in precast concrete structures. *Eng Struct*. 2017; 143: 306–315. doi:10.1016/j.engstruct.2017.04.028

[24] Beilic D, Casotto C, Nascimbene R, Cicola D, Rodrigues D. Seismic fragility curves of single storey RC precast structures by comparing different Italian codes. *Earthquakes Struct*. 2017; 12(3): 359–374. doi:10.12989/eas.2017.12.3.359

[25] Bournas DA, Negro P, Molina FJ. Pseudodynamic tests on a full-scale 3-storey precast concrete building: behavior of the mechanical connections and floor diaphragms. *Eng Struct*. 2013; 57: 609–627. doi:10.1016/j.engstruct.2013.05.046

[26] McKenna F. Opensees: a framework for earthquake engineering simulation. *Comput Sci Eng*. 2011; 13(4): 58–66. doi:10.1109/MCSE.2011.66

[27] Kent DC, Park R. Flexural members with confined concrete. *J Struct Div*. 1971; 97(7): 1969–1990.

[28] Scott RPBD, Priestley MJN. Stress-strain behavior of concrete confined by overlapping hoops at low and high strain rates. *J Proc*; 79 (1). doi:10.14359/10875

[29] Karsan ID, Jirsa JO. Behavior of concrete columns with double-head studs under earthquake loading: parametric study. *ASCE J Struct Div*. 1969; 95: 2543–2564.

[30] Menegotto M, Pinto PE. Method of analysis for cyclically loaded reinforced concrete plane frames including changes in geometry and non-elastic behaviour of elements under combined normal force and bending. In: Proceedings of the IABSE Symposium on the Resistance and Ultimate Deformability of Structures Acted on by Well Defined Repeated Loads, vol. 13, 1973; p. 15–22.

[31] Magliulo G, Ercolino M, Manfredi G. Influence of cladding panels on the first period of one-story precast buildings. *Bull Earthq Eng*. 2015; 13(5): 1531–1555. doi:10.1007/s10518-014-9657-2

[32] Belleri A, Torquati M, Marini A, Riva P. Horizontal cladding panels: in-plane seismic performance in precast concrete buildings. *Bull Earthq Eng*. 2016; 14(4): 1103–1129. doi:10.1007/s10518-015-9861-8

[33] Brunesi E, Nascimbene R, Bolognini D, Bellotti D. Experimental investigation of the cyclic response of reinforced precast concrete framed structures. *PCI J*. 2015; April. doi:10.15554/pcij.03012015.57.79

[34] Dal Lago B, Silvia L, Fabio B. Diaphragm effectiveness of precast concrete structures with cladding panels under seismic action. *Bull Earthq Eng*. 2019; 17(1): 473–495. doi:10.1007/s10518-018-0452-3

[35] Magliulo G, Ercolino M, Cimmino M, Capozzi V, Manfredi G. FEM analysis of the strength of RC beam-to-column dowel connections under monotonic actions. *Constr Build Mater*. 2014; 69: 271–284. doi:10.1016/j.conbuildmat.2014.07.036

[36] Magliulo G, Capozzi V, Fabbrocino G, Manfredi G. Neoprene–concrete friction relationships for seismic assessment of existing precast buildings. *Eng Struct*. 2011; 33(2): 532–538. doi:10.1016/j.engstruct.2010.11.011

[37] Fischinger M, Zoubek B, Isakovic T. Seismic behaviour of the beam-to-column dowel connections: macro modelling. *4th Int Conf Comput Methods Struct Dyn Earthq Eng COMPDYN 2013*. 2013; June: 1523–1532.

[38] Psycharis IN, Mouzakis HP. Shear resistance of pinned connections of precast members to monotonic and cyclic loading. *Eng Struct*. 2012; 41: 413–427. doi:10.1016/j.engstruct.2012.03.051

[39] Araújo M, Macedo L, Marques M, Castro JM. Code-based record selection methods for seismic performance assessment of buildings. *Earthq Eng Struct Dyn*. 2016; 45(1): 129–148. doi:10.1002/eqe.2620

[40] Fischinger M, Zoubek B, Isaković T. Seismic response of precast industrial buildings BT – perspectives on European earthquake engineering and seismology: volume 1. In: A. Ansal editor. Perspectives on European Earthquake Engineering and Seismology. Cham: Springer International Publishing, 2014; p. 131–177.

[41] Tzenov L, Sotirov BP, Boncheva P. Study of some damaged industrial buildings due to Vrancea. In: Proceedings of 6th ECEE Dubrovnik, vol 6, 1978; p. 59–65.

[42] Rodrigues H, Sousa R, Vitorino H, Batalha N, Varum H, Fernandes P. Characterisation of Portuguese RC precast industrial building stock. *Adv Civ Eng*. 2020; 2020: 7517205. doi:10.1155/2020/7517205